JOURNAL OF COMPUTATIONAL PHYSICS 108, 122–141 (1993)

A Hybrid Adaptive Gridding Procedure for Recirculating Fluid Flow Problems

D. LEE AND Y. M. TSUEI*

Institute of Aeronautics and Astronautics, National Cheng Kung University, Tainan, Taiwan, Republic of China

Received March 23, 1990; revised March 1993

A hybrid adaptive gridding procedure combining the concepts of both local grid refinement and global grid moving has been developed for time-independent recirculating flow problems. The procedure starts with the global grid moving method which provides an initial adaptive solution. Base on this initial solution, large error regions are flagged and local refinement is then applied on the large error regions. The methods for error estimation and interface treatment are discussed. The procedure is assessed in a one-dimensional convection-diffusion equation, a driven polar cavity flow, and a laminar backward-facing step flow. Efficiencies of the various approaches are evaluated. Specifically, in the test problems, the hybrid adaptive grid solution requires less than one-tenth of the CPU time of that of the uniform fine grid solution to achieve the same accuracy. The procedure can be conveniently extended to three-dimensional, irregular geometry flow problems.

INTRODUCTION

It is well known that the solution of a system of partial differential equations is strongly dependent upon the grid arrangement. In many cases, grid arrangement can affect not only the solution accuracy but also the numerical stability. In optimizing the grid distribution, the adaptive grid method [1–3] appears to be one of the most promising techniques. Adaptive methods have been applied to various topics including fluid, heat transfer, and combustion problems [4–23]. Adequate serveys and descriptions of this subject can be found in Refs. [1, 2].

Among various adaptive methods proposed, most of them can be roughly fitted into two categories [4]. The first category is the global refinement techniques which are represented by the variational method [12] and the equidistribution method [13–20] among others. In these methods, the total number of grid points is fixed and after adaption the grid points cluster in the regions where solution variations are large. The disadvantage of these methods lies in the shortage of grid points when the flow field is complicated. For example, if the grid is following one wave front and another one arises somewhere else, the initial grid then has to be adjusted abruptly [21]. As a consequence, certain solution accuracy can be lost.

The second category is the local mesh refinement methods which are represented by the works of Oliger and his co-workers [4, 5]. In this method, through the error estimation large error regions are flagged and several levels of grid refinement are applied in these regions to achieve the pre-set accuracy. Pattern recognition procedures and data structures are crucial to the success of these approaches. For problems with sharp wave fronts such as those with combustion or shock waves, many levels of grid refinement may be needed to obtain the desired resolution and complicated data structures may result.

Dannenhoffer [22] compared the above two approaches and concluded that both approaches are effective in reducing the solution error. Relative merits were discussed in his study. However, it was also stated that details in the implementation of each of the schemes make a detailed comparison impractical. The study suggested a combination of the two approaches to yield an optimum one. As also commented by Hedstrom and Rodrique [21], a technique which combines the best features of both the global and local methods is in high demand. Lee *et al.* [23] used a combined method of grid moving and local refinement in computing one-dimensional model equations. It was found that the combined method yielded a stable and accurate solution. Following the idea, in the present study the authors developed a hybrid adaptive gridding procedure for recirculating flow problems.

The grid addition technique of Smooke and Koszykowski [11] has partially adopted the hybrid gridding concept. In their study, a method which adds or deletes the grids (in contrast to moving base grids globally within the domain) to equidistribute a positive weight function over a given mesh interval in each direction was used. In this method,

* Current address: AIDC, Chung-Shan Institute of Science and Technology, Taichung, ROC.

0021-9991/93 $5.00

since the grids are added globally in each direction, some of the grid points may be wasted and this causes a loss of efficiency. On the other hand, because the computation is performed in the entire domain on a product grid, a sophisticated data structure can be avoided. Moreover, no treatment for the interfaces between the refined region and the base grid region is needed in this method. The refinement criteria of this method rest on the magnitude of the derivatives of selected flow properties.

In a very recent paper, an adaptive procedure was developed for convection diffusion problems by Acharya and Moukalled [25]. In their method, based on the values of the weight function obtained on the initial coarse grid, the regions which need refinement are flagged. The number of grid points in each flagged region is then increased and a new mesh based on variational principles is generated. The "inner" and "outer" solutions are iterated in a multi-grid fashion until convergence is obtained. Their procedure has been applied to three model problems with a very coarse initial grid. In their solutions, with the same amount of CPU time and a comparable accuracy to the finer uniform grid solutions, they found that a number of grid points could be reduced by three to five times. A close comparison between their procedure and the present one reveals the following differences: First, in the present study, the grid flagging is based on an adaptive solution (which is obtained by using the moving grid method) instead of an initial grid solution. Since an adaptive solution provides a more accurate basis, this practice is believed to significantly reduce the large error regions and refinement levels needed. Second, they used the weight function distribution as an indicator of the error distribution. This can be an alternative for a more sophisticated error estimator such as the Richardson method. However, the usefulness of this estimator should be further exploited. Third, a more sophisticated pattern recognition procedure and a more complicated data structure are needed to handle the highly irregular boundaries of their flagged regions. For a problem which requires multiple levels of refinement, the application of the procedure may not be straightforward. Lastly, the grid generation in the flaged region was based on a variational principle in their study. Two Poisson equations were solved to obtain their adaptive grid in the refined regions. For a three-dimensional application, computational overhead can be a major concern. More specific comparison of the two procedures will be addressed below.

In the present procedure, the grid moving method of Lee *et al.* [16, 17] is employed to obtain the initial adaptive solution. An error estimator is used to evaluate the truncation error at each adaptive grid node. The large error regions are then refined by using a denser grid (e.g., doubling the number of grid points). Boundary conditions for these refined regions are provided by the base grid solutions on the interfaces. Interactions between the "inner" (fine grid) solution and the "outer" (coarse grid) solution are checked to ensure that the solutions are consistent and converged in the entire domain.

As mentioned above, a direct comparison of the numerical efficiencies between the approaches of local refinement and global grid moving is difficult due to the wide variations in data structure, refinement criteria, details of the scheme implementation, and others. In this study, relative merits among schemes of local refinement, global grid moving and hybrid gridding are assessed only if ambiguity can be avoided. This means that the comparisons may not be general enough. The assessment of efficiencies of various approaches is based on the comparisons to the exact or very fine grid solutions.

GOVERNING EQUATIONS

In the present study, the two-dimensional, incompressible, laminar, recirculating flows have been used to demonstrate the usefulness of the technique. The general governing equations for the flows can be expressed in the following unified form as

$$\frac{\partial}{\partial t}(\rho\Phi) + \operatorname{div}(\rho V\Phi) = \operatorname{div}(\Gamma^{\Phi} \operatorname{grad} \Phi) + R^{\Phi}, \qquad (1)$$

where ϕ represents the dependent variable, Γ^{Φ} is the effective diffusion coefficient of variable ϕ, and R^{Φ} is a lumped source term for the equation. In order to handle the complex geometries, the above equation is transformed in a boundary-fitted coordinate system and this leads to the equation

$$\frac{\partial}{\partial t}(\sqrt{g}\,\rho\Phi) + \frac{\partial}{\partial q^j}(\sqrt{g}\,\rho V^j\Phi) = \frac{\partial}{\partial q^j}\left(\sqrt{g}\,g^{jk}\Gamma^{\Phi}\frac{\partial\Phi}{\partial q^k}\right) + \sqrt{g}\,R^{\Phi}, \qquad (2)$$

where V^j is the contravariant velocity, g^{jk} is the metric tensor, q^j and q^k are the general coordinates, and $\sqrt{g}$ is the Jacobian. For a two-dimensional, steady, incompressible flow, the governing equation becomes

$$\frac{\partial}{\partial\xi}(\sqrt{g}\,\rho U\Phi) + \frac{\partial}{\partial\eta}(\sqrt{g}\,\rho V\Phi) = \frac{\partial}{\partial\xi}\left(\sqrt{g}\,g^{11}\Gamma^{\Phi}\frac{\partial\Phi}{\partial\xi}\right) + \frac{\partial}{\partial\eta}\left(\sqrt{g}\,g^{22}\Gamma^{\Phi}\frac{\partial\Phi}{\partial\eta}\right) + S^{\Phi},$$

where

$$S^{\Phi} = \sqrt{g}\, R^{\Phi} + C^{\Phi}$$

$$C^{\Phi} = \frac{\partial}{\partial \xi}\left(\sqrt{g}\, g^{12} \Gamma^{\Phi} \frac{\partial \Phi}{\partial \eta}\right) + \frac{\partial}{\partial \eta}\left(\sqrt{g}\, g^{21} \Gamma^{\Phi} \frac{\partial \Phi}{\partial \xi}\right)$$

$$\sqrt{g} = x_\xi y_\eta - x_\eta y_\xi, \qquad g^{12} = g^{21} = -(x_\xi x_\eta + y_\xi y_\eta)/g$$

$$g^{11} = (x_\eta^2 + y_\eta^2)/g, \qquad g^{22} = (x_\xi^2 + y_\xi^2)/g$$

$$U = (uy_\eta - vx_\eta)/\sqrt{g}, \qquad V = (vx_\xi - uy_\xi)/\sqrt{g}. \tag{3}$$

Equations (3) can be discretized by using various differencing schemes such as the second-order upwind scheme and the power-law scheme (which is commonly used in the SIMPLE procedure [26]). The final form of the discretized equation is

$$A_\Phi \Phi_\Phi = \sum_{i = W,E,N,S} A_i \Phi_i + S. \tag{4}$$

The discretized momentum equation (4) along with a pressure correction equation are solved with the SIMPLE algorithm; details are discussed by Patankar [26].

NUMERICAL TECHNIQUES

1. Grid Moving Method

In the present grid moving method, weight functions constructed by using the flow property gradients are equidistributed. For example, along the x direction for the ith mesh

$$W_i \Delta x_i = \text{const.} \tag{5}$$

Therefore, for a large weight function W_i, the corresponding mesh size should be small to satisfy the above relation.

To improve grid quality, the weight function used by Dwyer *et al.* [13] is modified to account for the coupling of the weight functions among the neighboring grid points. The modified W at the grid (i, j) along x direction assumes the form of [16, 17, 20]

$$W_{i,j} = 1 + \sum_N b_N \left[|\phi_\xi|_{i,j} + \sum_{k=1, k\neq i}^{m} |\phi_\xi|_{k,j}\, xC_t \exp(-|i-k|) + \sum_{l=1, l\neq j}^{n} |\phi_\xi|_{i,l}\, xC_t \exp(-|j-l|) \right], \tag{6}$$

where b is a weighting parameter, N is the number of property gradients considered, ϕ_ξ is the gradient of the property ϕ along the ξ line, and C_t is the coupling coefficient. With $C_t = 0$ weight functions decouple from each other and resume the original form of that used by Dwyer. In the present study, C_t is set to unity. It has been shown in other studies [16, 17] that the coupling of weight functions can improve the grid quality and result in a more accurate solution.

To construct a product adaptive grid, the initial grid (e.g., a uniform grid) solution is first obtained. Using this solution, the property gradients in the weight functions are calculated and these weight functions are then used to redistribute the grid according to Eq. (5).

2. Truncation Error Estimation

Error estimation is one of the most important steps in applying a local refinement method. This step shall identify the regions which need refinement. Very often, the method of Richardson extrapolation [4, 5, 27, 28] is used to estimate the solution error. This method requires computation of flow field twice, once on a fine grid, the other on a coarse grid (e.g., doubling the mesh size of the fine grid), and the solution differences are taken as an indicator of the error. There are advantages to this method [5], for example, it is independent of the PDE as well as the difference scheme. Nevertheless, we found a direct estimator based on the current solution is preferable if it exists, since the procedure can then be simplified especially when a three-dimensional problem is treated. In a nonuniform grid (as in an adaptive grid) the application of the Richardson method is not as convenient as it is in a uniform grid. In a uniform grid, to apply the method, a common practice is to double the mesh size so that a coarser grid solution can be obtained on the base grid, and an extrapolation formula (e.g., Eq. (8a) in Ref. [4]) is then applied. Note that this formula is based on a uniform grid size in one dimension so that the denominator is $2^p - 1$, where p is the order of the method. In a nonuniform grid, based on the local grid size, the denominator of this formula should be replaced by $R^p - 1$, where R is the ratio of the neighboring grid sizes. The ratio changes from grid point to grid point and needs to be evaluated. This requires extra computation and should affect the accuracy of the formula too. If the method is carried out by halving the grid size, this problem can be avoided. However, since the grid is doubled, it ends up using a denser grid for the error estimation, and this extra computational effort should be taken into account. In this study, we double the number of grid points in the method.

As an example of the direct method, in this study, a formula which was developed by the authors [24] for a direct estimation of truncation error is employed. This formula is based on the truncation error of convection terms in a curvilinear coordinate system. The formula takes the form

$$T_E = T_{E1} + T_{E2} + T_{E3}, \tag{7}$$

where

$$T_{E1} = -\frac{\rho}{2J}\left[(Ux_{\xi\xi\xi} + Vx_{\eta\eta\eta})\, f_x + (Uy_{\xi\xi\xi} + Vy_{\eta\eta\eta})\, f_y\right] \quad (8)$$

$$T_{E2} = -\frac{\rho}{J}\{(Ux_\xi x_{\xi\xi} + Vx_\eta x_{\eta\eta})\, f_{xx} + [U(y_\xi x_{\xi\xi} + x_\xi y_{\xi\xi}) + V(y_\eta x_{\eta\eta} + x_\eta y_{\eta\eta})]\, f_{xy} + (Uy_\xi y_{\xi\xi} + Vy_\eta y_{\eta\eta})\, f_{yy}\} \quad (9)$$

$$T_{E3} = -\frac{\rho}{3J}\left[(Ux_\xi^3 + Vx_\eta^3)\, f_{xxx} + 3(Ux_\xi^2 y_\xi + Vx_\eta^2 y_\eta)\, f_{xxy} + 3(Ux_\xi y_\xi^2 + Vx_\eta y_\eta^2)\, f_{xyy} + (Uy_\xi^3 + Vy_\eta^3)\, f_{yyy}\right]. \quad (10)$$

In these equations, ρ is density, J is the Jacobian, U, V are the contravariant velocities, f represents the flow properties such as primary velocities u, v. In using Eq. (7) as a truncation error estimator, it has been assumed that in the computation that the truncation error of the convection terms is dominant. In the following test cases, this formula is found to perform satisfactorily. The resulting flagged regions are comparable to those obtained by using the Richardson method. Since the formula is employed only as an error indicator, the accuracy of its value is not a primary concern. The computational overhead for the error calculation is minor since in this formula all item values except f derivatives are readily available at each grid.

In our opinion, both the Richardson method and the formula should be used only as error "indicators" rather than value "estimators" since neither can provide exact values of errors in all cases. This statement is further justified in the test cases.

In the Richardson method, when the normalized solution error exceeds a pre-assigned value (e.g., 0.015), the grid is flagged. For the truncation error formula, the grid is flagged if its normalized truncation error exceeds a pre-assigned value (e.g., 0.1). The definition of the normalized truncation error is

$$\bar{T}_E = \frac{|T_E|}{|T_E|_{\max}}. \quad (11)$$

Since T_E can be either positive or negative, absolute values should be used. The selection of the pre-assigned values is relatively arbitrary. However, too small a value usually results in too large a flagged region and more unnecessary computation. On the other hand, too large a pre-assigned value causes a small flagged region, together with inaccurate internal boundary conditions. Iterations between the "inner" and "outer" solutions will be necessary. This may result in efficiency loss.

3. Interface Treatment and Solution Iteration

Location of the internal boundary can determine the necessity of the iteration between the "inner" and "outer" solutions. Internal boundary conditions for the flagged regions are specified by using the base grid solution. In a limiting case, if the interface has the exact values no solution iteration will be needed theoretically. In practice, the interfaces should be placed in a region (if there is one) where the solution is accurate to a certain degree. Based on this viewpoint, it is believed that too coarse an initial grid results in a strong requirement for the solution iteration, since the boundary conditions (which is prescribed by the initial grid solution) for the flagged regions may never be accurate. In other words, the flagging criteria should be reasonably loose so that the interface can be located in a region which contains an accurate solution.

In the procedure, the internal boundary for the refined region is set two grid widths toward the low error region from the original boundary which is "flagged" by the error indicator. By doing so, it was shown in the test problems that, due to these more accurate boundary conditions, the errors in the refined regions were reduced. Also, we found that the iterations between the "inner" and "outer" solutions mentioned in Ref. [4] were not needed in some of our test problems. In other studies by the authors, only one iteration cycle was needed in most cases.

Along an interface, interpolation is required to transfer the solution from the coarse to the fine grid or vice versa to provide boundary conditions for the other region. The conservative interpolation technique of Rai [29] is adopted in this study. This technique requires that, across a segment of the interface, the fluxes of both sides of the interface should be equal [30]. Therefore, with known fluxes from one side, variables at each grid node along the boundary can be obtained accordingly, and flux conservation is automatically assured. In our study, since grid size is halved to refine the grid, interpolation is relatively easy.

4. Solution Procedure

The general procedure of the present hybrid method follows the steps below:

1. Obtain the initial base grid solution.
2. Calculate the weight function defined in Eq. (6) at each grid and construct the adaptive grid according to Eq. (5).
3. Obtain the initial adaptive grid solution.
4. Obtain the error distribution by using one of the error indicators.
5. Flag the larger error regions; select the boundaries for the flagged regions. A buffer zone is applied between the coarse grid region and the flagged region.

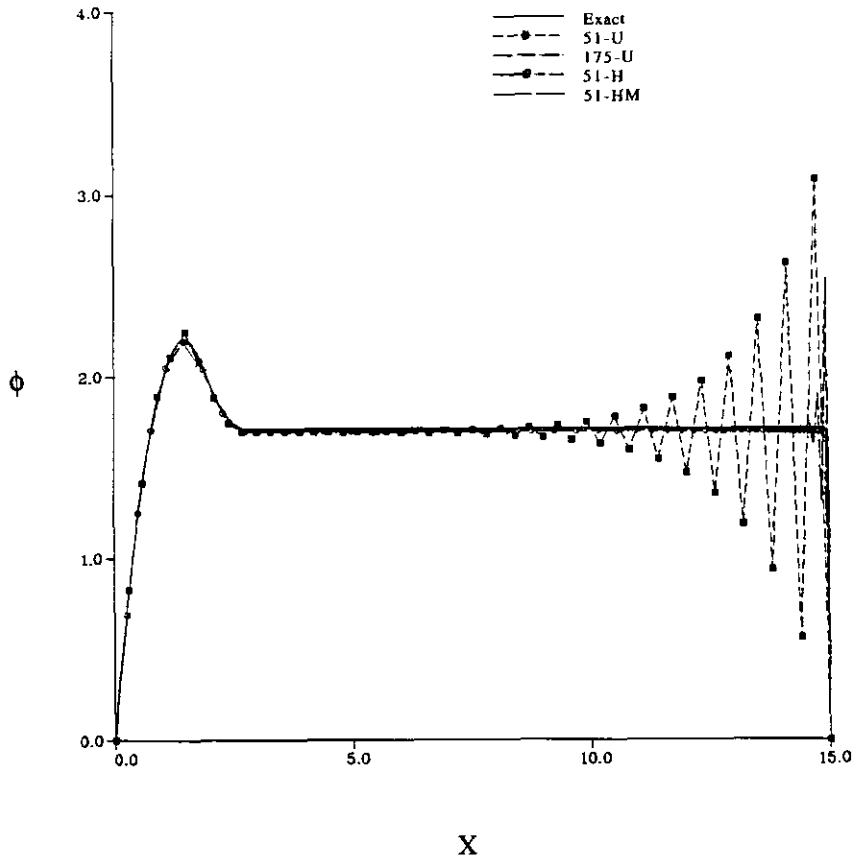

FIG. 1. Solutions of the one-dimensional convection-diffusion equation (second-order central difference).

6. Apply a finer mesh in the flagged regions.

7. Use the base grid solutions to specify the boundary conditions for the flagged regions.

8. Re-calculate the solution in each flagged region.

9. Along the interfaces (which are inside the flagged regions) of the coarse grid regions, interpolate the fine grid solution to specify the boundary conditions for the coarse grid regions.

10. Re-calculate the coarse grid solution. If the overall normalized solution change is larger than a specified percentage, repeat steps 7–10 until the criteria are met.

11. Advance to the next level of refinement if required.

A few comments may be useful to clarify the steps. Grid moving (steps 2–3) before a local refinement is believed to be one of the most important features of the method. Through these steps, the large error region can be reduced due to the improved adaptive solution. This effect is shown in Fig. 1. This reduction of large error region can be significant in a three-dimensional problem. Grid resolution in high gradient regions also significantly increases after one round of grid moving as can be seen in Table I. The finest grid size (0.1) is only one-third of the initial grid size.

In step 4, when the Richardson method is applied to an adaptive grid, our practice is to halve the grid size instead of halving the number of grid points. However, this will require the computation of a dense grid solution. If the formula (or other direct estimator) is employed, errors can

TABLE I

Summary of the Performances of the Various Approaches (with Second-Order Central Difference)

Case	ERR_t	G.S.	Grid
51-U	2.63	0.3	51
51-M	0.69	0.1	51
51-H	0.21	0.05	85
51-HM	0.15	0.04	85
85-M	0.39	0.05	85
101-U	0.65	0.15	101
125-U	0.42	0.12	125
151-U	0.28	0.10	151
175-U	0.21	0.08	175
201-U	0.17	0.07	201
501-U	0.03	0.03	501

Note. U = uniform grid; M = moving grid; H = hybrid grid; HM = hybrid grid with moving grid refinement; G.S. = finest grid size; $ERR_t \equiv \sum_{i=1}^{N} |\phi - \phi_{exact}|_i \Delta x_i$.

be evaluated directly at each grid point using the current solution without solving for a second solution. In step 6, to refine the grid in the flagged regions, two approaches are compared in this study. The first approach is simply halving the grid size (H grid), and the other is using this doubled number of grid points and applying the grid moving method in the flagged regions again (HM grid). In this study, the H grid will be the standard practice for all the test problems. The HM grid is used only in the polar cavity flow to assess its usefulness.

Although the procedure is not limited to one level of refinement, excessive levels of refinement will require a sophisticated pattern recognition procedure and the resulting data structure will be complicated. This is undesirable for a practical engineering application. In the present study, assessments are based on one level of refinement.

5. Solver

This study employed the well-known SIMPLE algorithm [26] in a boundary-fitted coordinate with a non-staggered grid arrangement. In the two-dimensional test problems, second-order upwind and second-order central schemes are used in discretizing the convection terms and diffusion terms, respectively. Primary velocities have been chosen as dependent variables. The detailed formulation was discussed by Lee *et al.* [31, 32]. All the computations in this study were performed on a DIGITAL VAX8600 computer.

TEST PROBLEMS AND RESULTS

In this section, three prototype problems have been used to demonstrate the applicability of the procedure. The first is a one-dimensional convection-diffusion equation with a source term [14, 23]. The results are compared to the exact solution. In this problem, features of the present adaptive procedure are clearly demonstrated. The second problem is a laminar driven polar cavity flow with a Reynolds number of 350. The hybrid adaptive solution of this problem is compared to a very fine uniform grid solution, viz. 129×129, which mimics the experimental data of Fuchs and Tillmark [33] closely. The third one is a laminar backward facing step flow with a Reynolds number of 800. Here, a 101×101 uniform grid solution has been used as a reference solution. In the study, comparisons are based on the solutions driven to the same level of convergence. The convergence criteria for the two-dimensional problems are that the normalized maximum residuals of both momentum and continuity equations in the domain be less than 10^{-6}.

For the test problems, the deviation from a reference solution is used as a measurement of the accuracy of the methods. Two of these solution errors, the normalized mean error ERR and the normalized maximum error $\mathrm{ERR}_{\max}$ are defined in the following and used in the test problems.

$$\mathrm{ERR} = \frac{1}{N}\sum_{i=1}^{N}\left[\frac{\sqrt{(u-u_0)^2+(v-v_0)^2}}{\sqrt{u_0^2+v_0^2}}\right]_i \times 100\% \tag{12}$$

$$\mathrm{ERR}_{\max} = \max_{i=1}^{N}\left|\frac{\sqrt{(u-u_0)^2+(v-v_0)^2}}{\sqrt{u_0^2+v_0^2}}\right|_i \times 100\%, \tag{13}$$

where u, v are the coarse grid velocities and u_0, v_0 are the fine grid reference solutions. For all the test cases, the efficiency of the adaptive procedure, rather than the details of flow physics, has been emphasized.

1. One-Dimensional Convection-Diffusion Equation with a Source Term

Consider the following model equation [14, 23],

$$u\phi_x = v\phi_{xx} + S(x), \qquad u, v = \text{const} \tag{14}$$

with the source term,

$$\begin{aligned} S(x) &= cx + d, && 0 \leqslant x \leqslant x_1 \\ &= -\frac{cx_1+d}{x_2}x + \frac{cx_1+d}{x_2}(x_1+x_2), && x_1 \leqslant x \leqslant x_1+x_2, \end{aligned} \tag{15}$$

where $c = -2.0$, $d = 3.0$, $x_1 = 2h$, $x_2 = h$, and $h = \frac{15}{16}$. The overall Peclet number $uL/v = 1000$, where the total length L is 15 in the problem.

Given the boundary conditions $\phi(0) = 0$ and $\phi(L) = 0$, the exact solution of Eq. (13) is depicted as the solid line in Fig. 1. The exact solution shows that besides having a region where the convection term is balanced by the source term, there also exists a boundary layer where the convection term is balanced by the diffusion term only. This boundary layer requires a large number of grid points to obtain an accurate solution. In this problem, we first used the second-order central scheme for both the convection and diffusion terms. As is well known, there exist wiggles in the solution if the local Peclet number is greater than two. To suppress solution wiggles, 500 uniform grids will be needed in this problem. In a second test, a first-order upwind scheme is used to discretize the convection term, and a second-order central scheme is used for the diffusion term. The solution is wiggle-free but less accurate. It was shown that the hybrid procedure can effectively improve the solution in both tests.

Central Differences

For the first test, the errors of solutions of the 51 uniform grid and the adaptive grid (with grid moving method) are

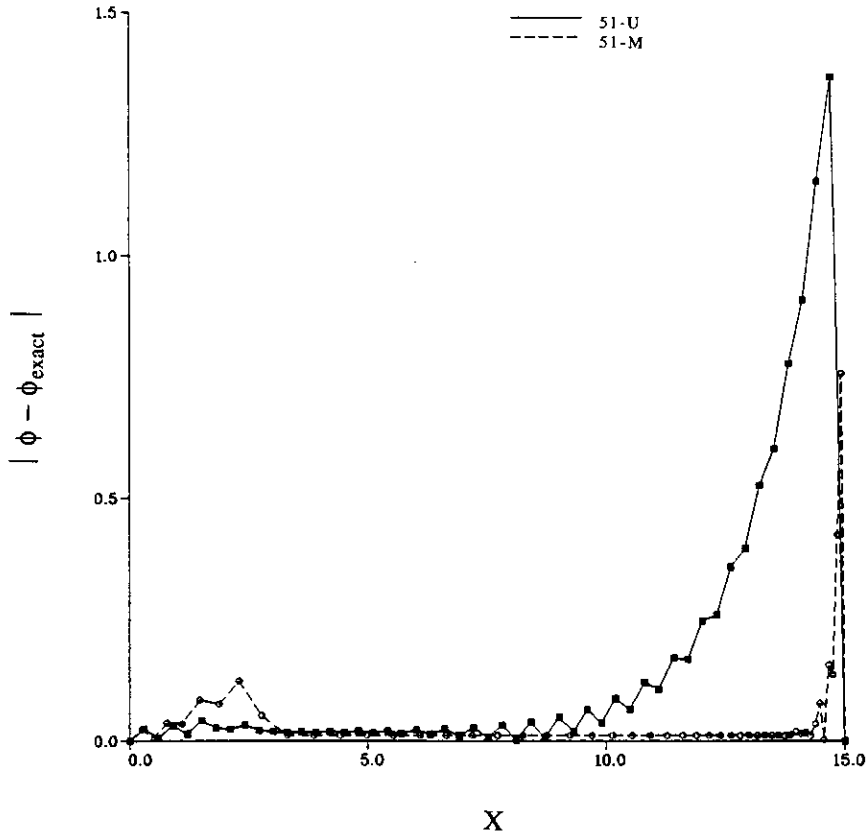

FIG. 2. Solution errors of the uniform grid and adaptive grid solutions.

compared in Fig. 2. It is obvious that the large error regions and the maximum error are significantly reduced in the adaptive solution. If the uniform grid solution error were used to flag the large error regions, there would be only one region which is much wider than those obtained by using the grid moving solution, as is seen in the figure. Consequently, more grid points and/or more levels of refinement will be needed for the uniform grid case to obtain similar resolution to that of the grid moving one. To flag large error regions of the adaptive solution, the truncation error formula in one-dimensional form was also used. Figure 3 compares the error distribution obtained by the Richardson method and the formula with the exact solution error distribution. The figure is blown up near the boundary layer. In the figure, errors are normalized by the peak error. The formula adequately indicates the large error regions in this problem. Note that the formula provides truncation errors in contrast to solution errors by the Richardson method. Both of the methods are intended to be used as the error indicators only.

Following the procedure, the number of grid points in the flagged regions is doubled. The resulting solutions using various approaches are shown in Fig. 1 already. In these solutions, since the second-order central scheme is used for the convection term, very strong wiggles appear in the uniform grid solutions even with 175 grid points. On the other hand, the hybrid adaptive solutions are wiggle-free as seen in Fig. 4. The bondary layer region of the solutions is shown in Fig. 4. The best solution is due to the hybrid method with the HM grid. To compare the performances, Table I summarizes the total error, the total number of grid points used, and the finest grid size of the various approaches. The hybrid methods use a total grid points of 85. With this number of grid points the grid moving method can achieve the accuracy of that of the 125 uniform grid point solution. The hybrid methods, on the other hand, can achieve the accuracy of that of the 175 and 201 uniform grid point solutions, respectively. Also note that the finest grid size of the HM grid is 0.04 which is about one-eighth of the initial uniform grid size. For a local refinement method, three levels of refinement will be needed to achieve the same grid size if halving the grid size is used in the refinement procedure. Note that the solution profile of the HM grid in the "boundary layer" region is almost perfect in this case. The HM grid is believed to be effective in a region which contains strong property gradients.

The "inner" and "outer" solutions iteration is found to be unnecessary in the present case. The reason can be

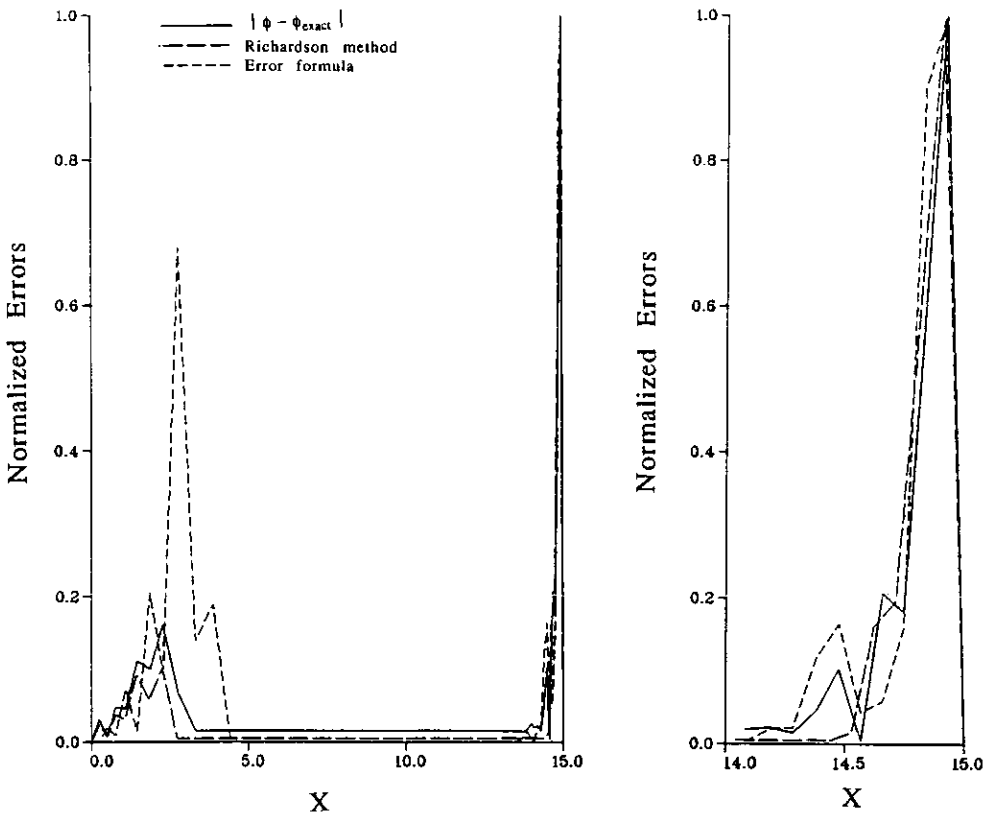

FIG. 3. Error distributions obtained from various error indicators.

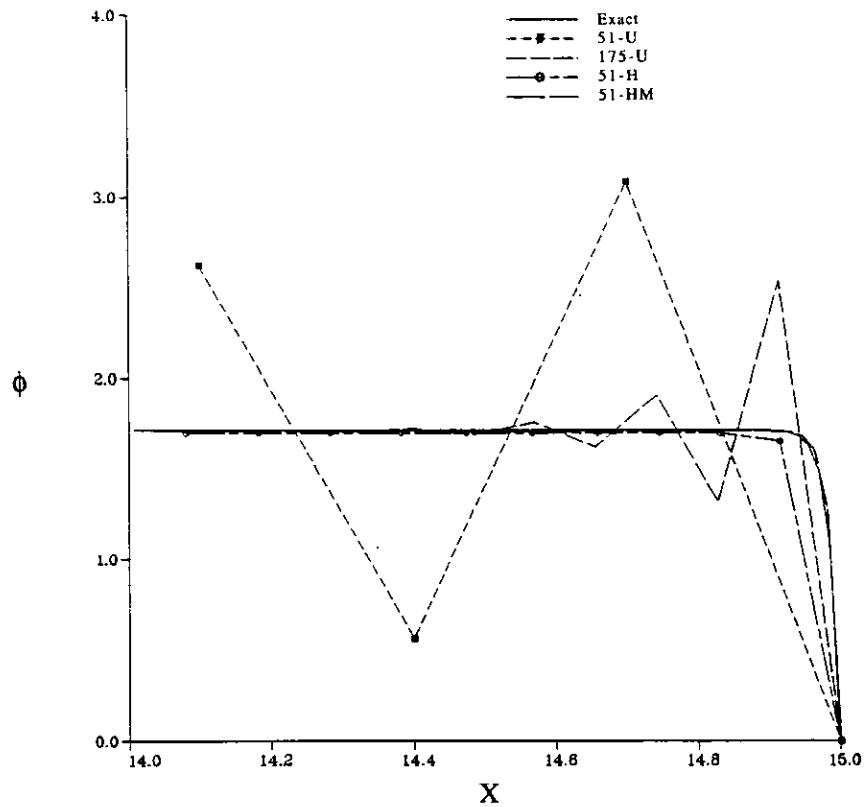

FIG. 4. Solutions near boundary layer region.

attributed to the accurate solution values of the interfacial boundary which is located in the low error, flat solution region.

Upwind Differences

For the second test, the first-order upwind scheme is employed for the convection term. A similar procedure as used in the previous case is followed except that in the flagged regions the number of grid points is increased to eight times that of the base grids. This is because an inaccurate scheme is employed, and more grid points are expected to be needed to achieve an accurate solution. Error distributions are displayed in Fig. 5. The large solution error region flagged by the Richardson method is wider. Therefore, the entire domain will need refinement. After refinement, it is found that many grid points in the flat solution region are wasted. On the other hand, the truncation error formula indicates a flagged region which is more concentrated in the "error source" region. These flagged regions which need refinement are smaller. In this test case, large errors stem from the region where the source term dominates, and these errors are carried downstream. If the solution in this region is improved, the downstream solution can be improved after one cycle of solution iteration without increasing the number of grid points in the flat solution region. The following results are based on the flagged regions obtained by the formula instead of that obtained by the Richardson method. Figure 6a shows the solutions of the various approaches. The solutions in the boundary layer region are clearly depicted in Fig. 6b. In contrast to the previous test case, since the initial grid provides an inaccurate solution everywhere in the domain, a solution iteration (steps 8–10) should be expected due to the inaccurate boundary conditions for the large error region. In this test case only one cycle of iteration is employed.

Table II summarizes the performance of each method. In this table, G.S.1 represents the finest grid size in the first large error region, where the source term dominates, and G.S.2 stands for the finest grid size in the second large error region, where the solution boundary layer occurs. The best gridding method in this case is the H grid method. This grid yields a solution comparable to that of the 1501 uniform grid. Although the finest grid size in either of the large error regions is smaller than that of the H grid, the HM grid does not yield the best solution. This is probably due to the feature of the present grid moving method. Since the weight functions use only the first derivatives, it cannot properly

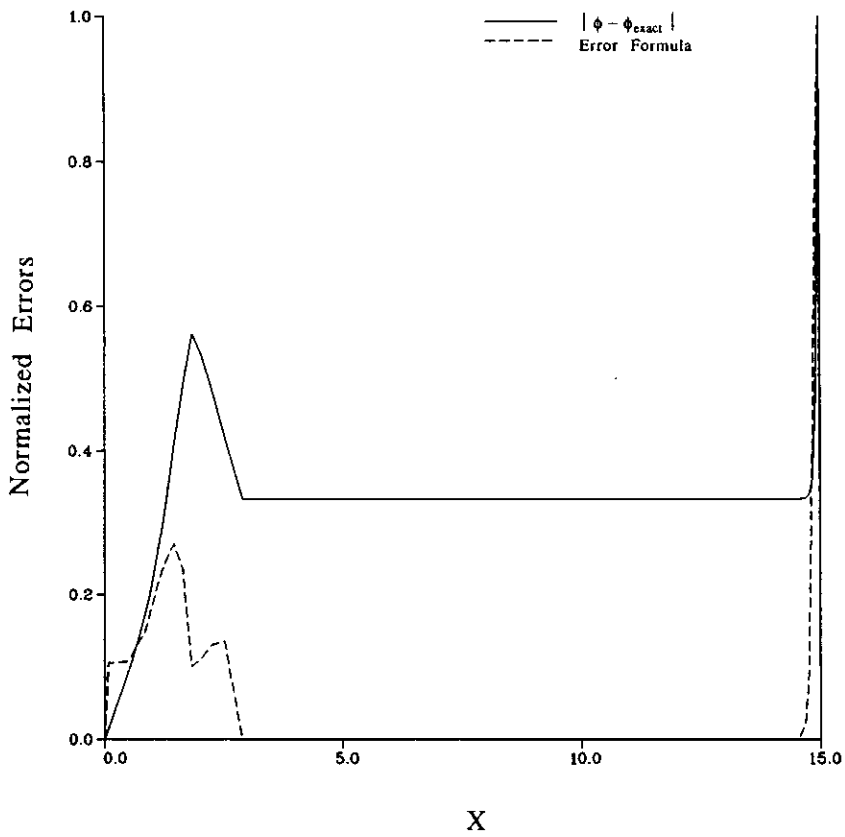

FIG. 5. Error distributions (first-order upwind scheme).

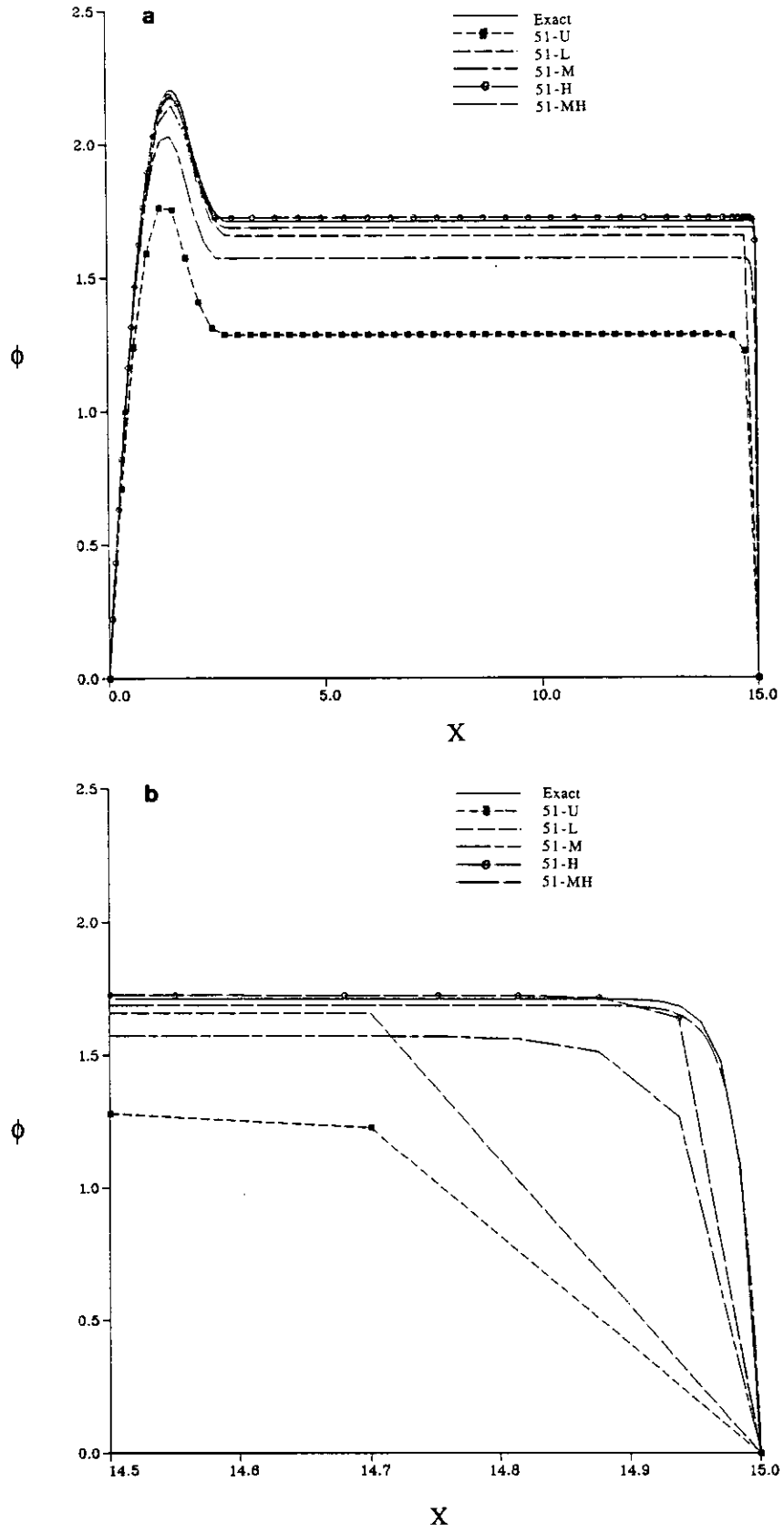

FIG. 6. (a) Solutions of the one-dimensional convection-diffusion equation (first-order upwind difference). (b) Solutions near the boundary layer.

TABLE II

Summary of the Performances of the Various Approaches (with First-Order Upwind Difference)

Case	ERR_f	G.S. 1	G.S. 2	Grid
51-U	6.25	0.3	0.3	51
51-M	2.11	0.077	0.062	51
51-L	0.80	0.0375	0.0375	216
51-H	0.22	0.0111	0.0078	277
51-HM	0.29	0.0073	0.0038	277
277-M	0.51	0.011	0.0052	277
151-U	2.14	0.1	0.1	151
301-U	1.09	0.05	0.05	301
401-U	0.82	0.0375	0.0375	401
501-U	0.66	0.03	0.03	501
751-U	0.44	0.02	0.02	751
1001-U	0.33	0.015	0.015	1001
1151-U	0.29	0.013	0.013	1151
1251-U	0.26	0.012	0.012	1251
1501-U	0.22	0.01	0.01	1501
1751-U	0.19	0.0086	0.0086	1751
2001-U	0.16	0.0075	0.0075	2001

Note. U = uniform grid; M = moving grid; L = local refinement; H = hybrid method; MH = hybrid method with moving grid; G.S. = finest grid size; $ERR_f \equiv \sum_{i=1}^{N} |\phi - \phi_{exact}|_i \Delta x_i$.

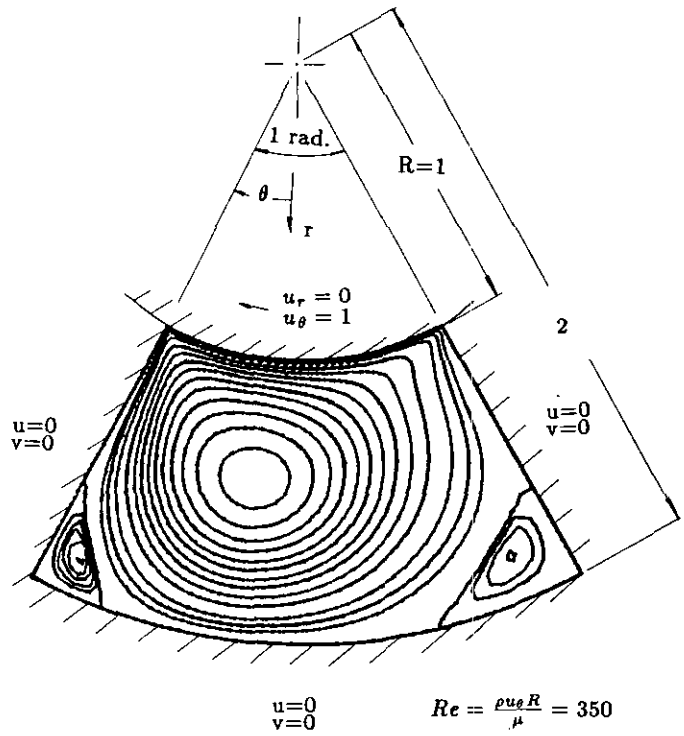

FIG. 7. Polar cavity flow with the boundary conditions.

resolve the region where the solution has a zero property gradient; even the finest grid size is smaller. The error from this region is carried downstream and causes a higher overall error. Nevertheless, the HM grid acquires a much better solution profile in the boundary layer region as is shown in the same figure. Note that the total grid points employed in the H grid are 277. This number of grid points, if used in a grid moving method, can achieve an accuracy comparable to that of the 700 uniform grid. For the basic local refinement method (51L) with one level of grid refinement ($\times 8$), total grid points of 216 yield a solution accuracy of that of the 401 uniform grid. This similar accuracy is expected since the finest grid sizes in both cases are similar. Note that the flagged regions are wider in this case. Because they are based on the initial uniform grid solution which is less accurate than the moving grid solution.

2. Driven Polar Cavity

A lid-driven polar cavity flow with a Reynolds number of 350 is used to assess the procedure. This problem has been studied experimentally as well as numerically by Fuchs and Tillmark [33]. The numerical and the experimental results were found to be in very good agreement in their study. The physical dimensions and boundary conditions are shown in Fig. 7. Also shown in the figure are the streamlines. It was demonstrated by the present author in another study [16] that our 81×81 fine grid solution mimicked the experimental data of Fuchs and Tillmark [33] closely. In this study, the solution of an even finer grid of 129×129 was chosen as the reference solution for comparison. The base grid used in this problem is 25×25. With this base grid solution, the grid moving method is applied first to obtain the initial adaptive grid solution (case 25-M in Table III). At this stage, the error has been reduced to one-third of that of a uniform grid solution with a computational overhead of less than 20%

TABLE III

Summary of the Performances of the Various Approaches (Polar Cavity Flow)

Case	ERR	ERR_M	CPU	Grid	G.S.(ξ, η)
25-U	32.6	96.6	131	625	(0.033, 0.040)
25-M	10.7	38.1	151	625	(0.018, 0.021)
25-H	3.0	9.8	451	882	(0.009, 0.011)
25-HM	2.8	9.5	497	882	(0.005, 0.007)
31-U	20.3	61.9	266	961	(0.026, 0.033)
31-M	7.0	24.5	280	961	(0.014, 0.017)
41-U	11.8	35.9	795	1681	(0.020, 0.025)
41-M	4.0	13.5	892	1681	(0.011, 0.013)
61-U	5.2	16.1	3580	3721	(0.013, 0.017)
61-M	1.8	6.7	3701	3721	(0.007, 0.008)
81-U	3.1	10.0	32900	6561	(0.010, 0.013)
101-U	2.0	6.0	115200	10201	(0.009, 0.010)
129-U	—	—	499562	16641	(0.006, 0.007)

Note. U = uniform grid; M = moving grid; H = hybrid method.

(Table III). Note that this adaptive solution has an accuracy comparable to that of a 41×41 uniform grid solution. In the next step, the large error regions of the initial adaptive solution are flagged by employing both the Richardson method and Eq. (7). Figure 8 shows these large error regions flagged by the various indicators. The full marks represent the large error grid nodes in the θ-direction velocity, and the open circles stand for the large error grid nodes in the r-direction velocity. The large solution error regions of the initial adaptive solution are shown in Fig. 8a. Grid points are flagged whenever the normalized solution error relative to the fine grid solution is larger than 0.015. Note that the solution error is normalized by the top wall velocity which is unity in this case. As mentioned before, a key step in the present procedure is the use of a moving grid solution as the base for flagging the grid points. If the initial uniform grid solution is used, the large error regions will be much broader, as shown in Fig. 8b. The same flagging

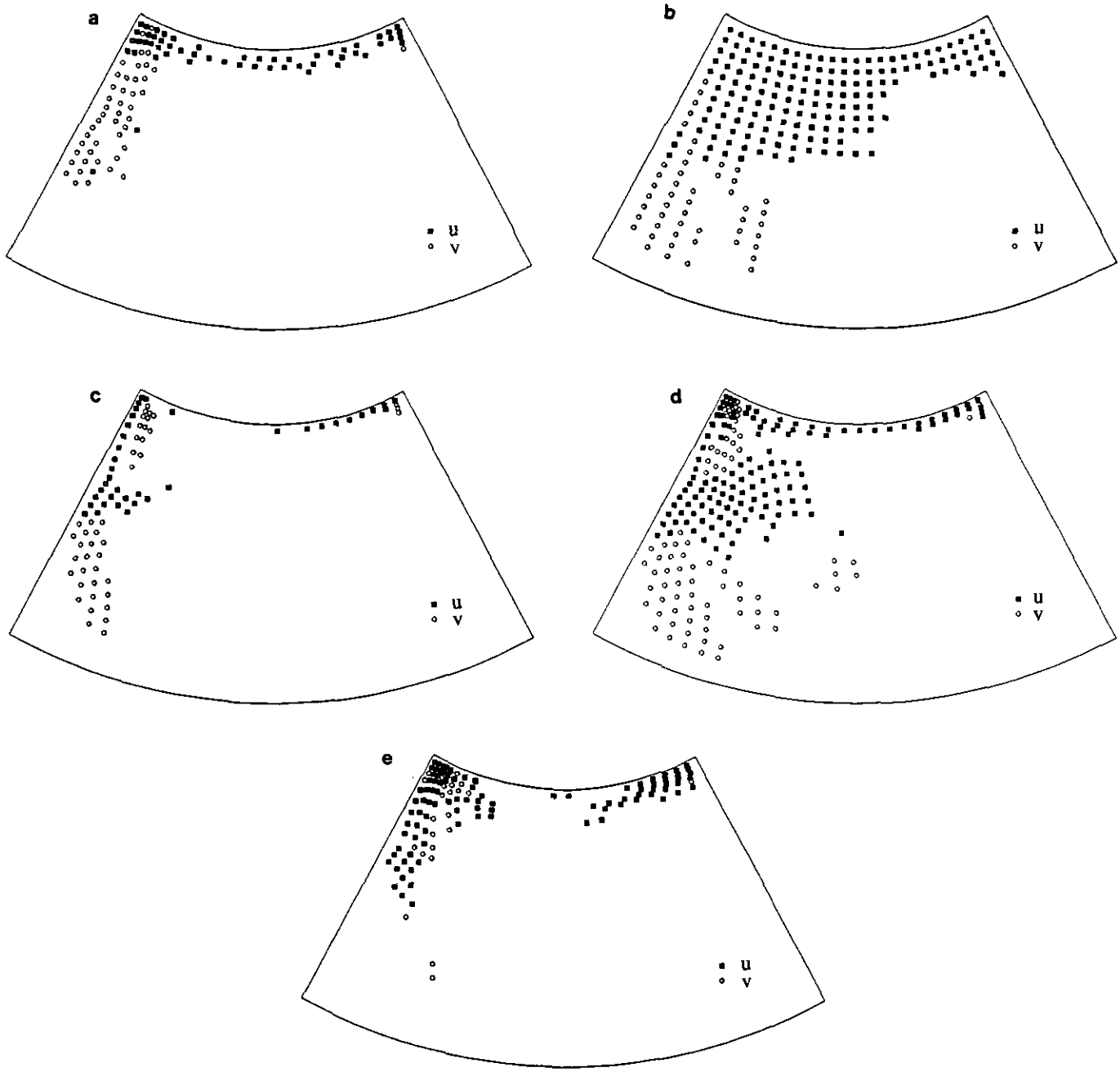

FIG. 8. Large error regions flagged by the various indicators: (a) based on the initial adaptive grid solution (0.015); (b) based on the initial uniform grid solution (0.015); (c) by the Richardson method (0.025); (d) by the Richardson method (0.015); (e) by the formula Eq. (7) (0.1).

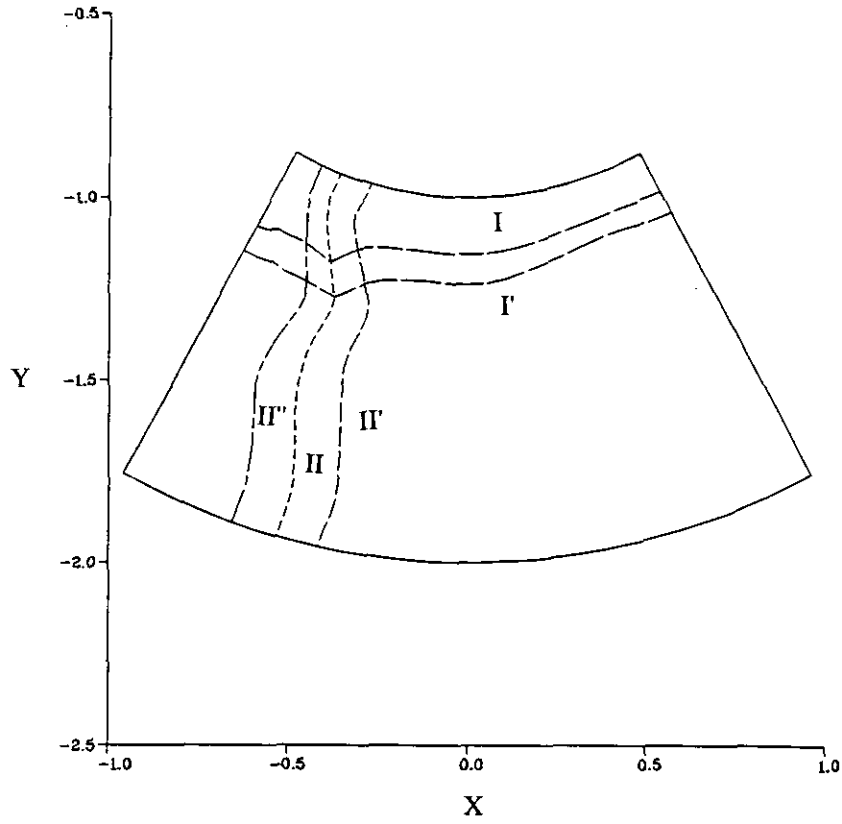

FIG. 9. Internal boundaries in the polar cavity problem.

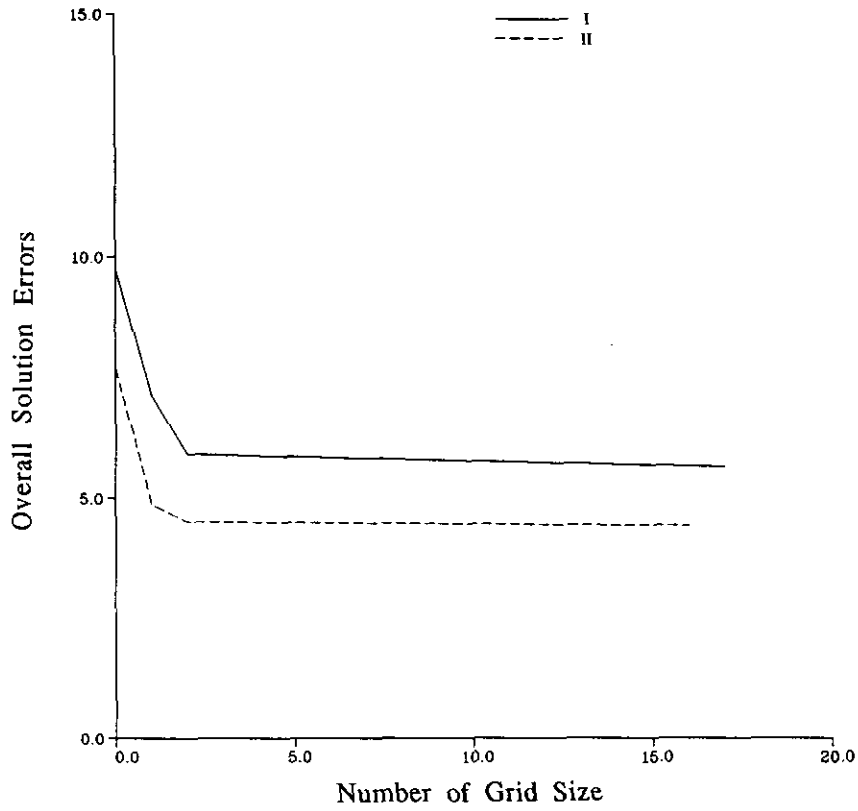

FIG. 10. Effect of the internal boundary location.

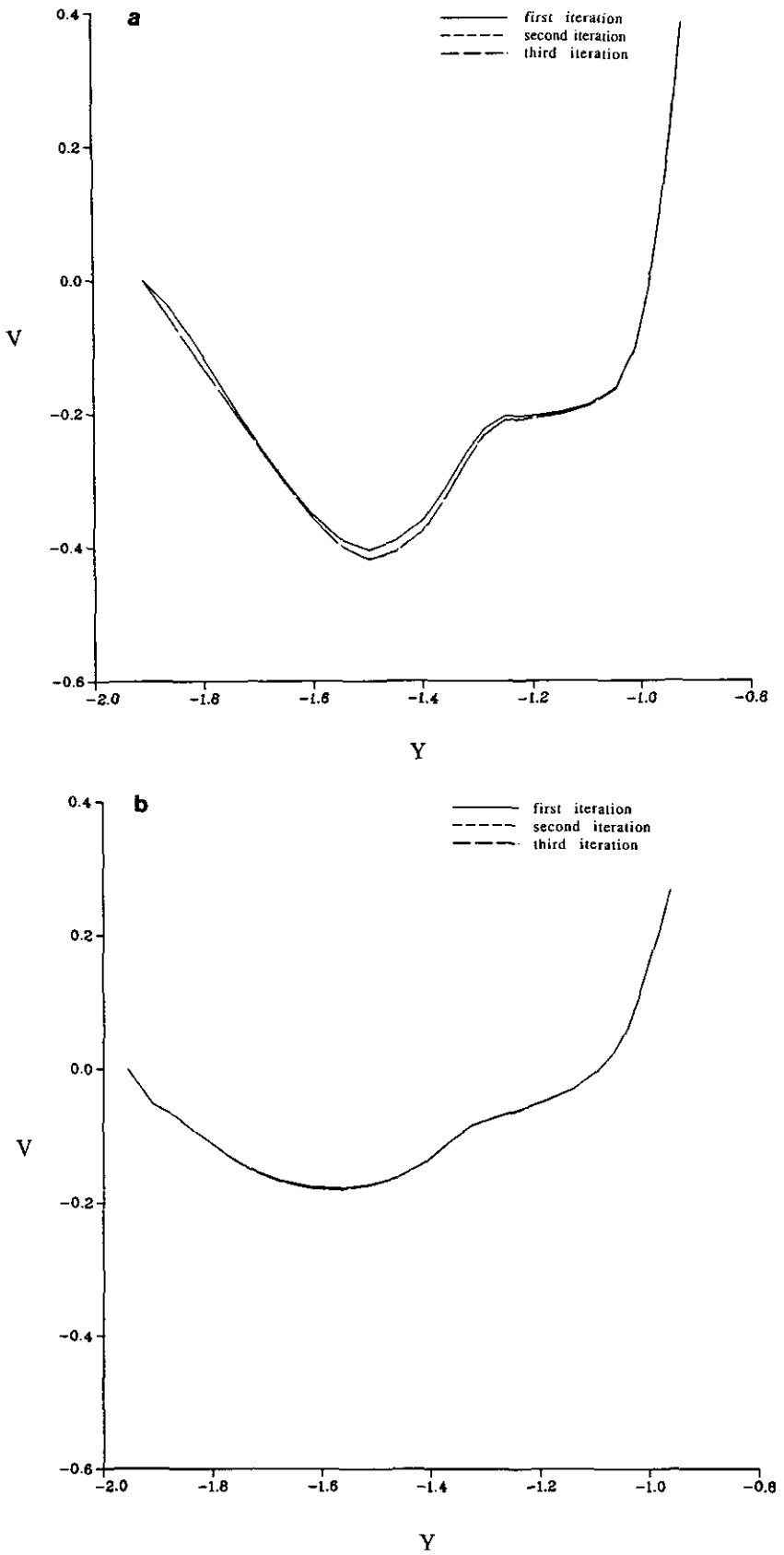

FIG. 11. The velocity profiles along the boundaries II″ and II′ in Fig. 9: (a) along II″; (b) along II′.

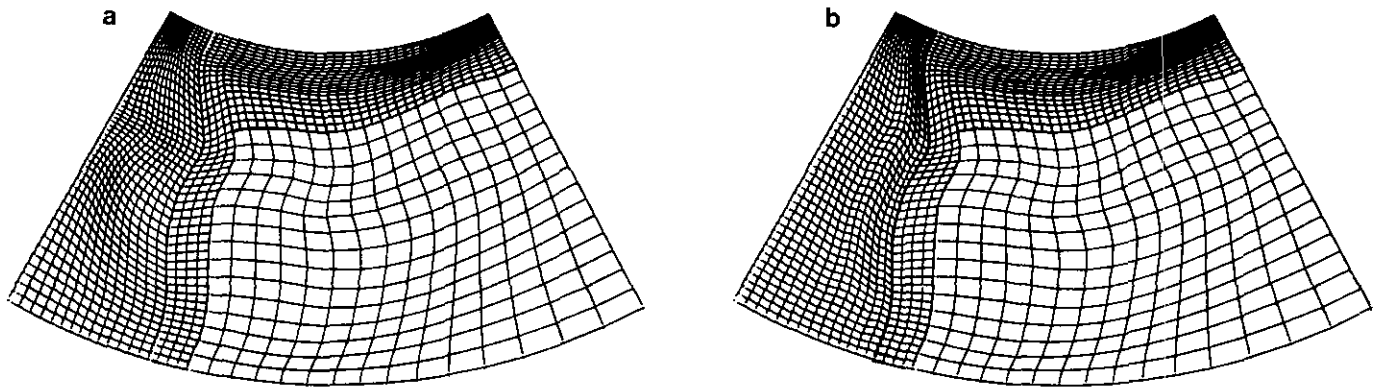

FIG. 12. The adaptive grids for the polar cavity flow: (a) H grid; (b) HM grid.

criterion is used in both cases. Obviously, less effort for subsequent grid refinement will be needed when using an adaptive initial solution. Figure 8c demonstrates the results obtained by the Richardson method with a flagging criterion of 0.025. If the same criteria as that used in Figs. 8a and b are employed, the flagged region will be much wider, as shown in Fig. 8d. In Fig. 8e, the formula is used. Grid points are flagged whenever the normalized truncation error $\bar{T}_E$ (Eq. (11)) is larger than 0.1. Qualitatively, both the flagging methods are useful. After flagging the large error regions, the number of grid points in these regions is doubled. The effects of the location of an internal boundary are discussed below.

In Fig. 9, I and II are the boundaries of the original flagged region. In the procedure, these boundaries are extended two grid sizes toward the lower error region to the lines I′ and II′. The effect of the location of the boundaries on the flagged region solutions is shown in Fig. 10. When the boundaries move outward two grid sizes or more, the overall solution errors of the refined regions remain unchanged. This result demonstrates the effect of the choice of internal boundary location. This explains why the iteration between the "inner" and "outer" solutions is not needed in this specific problem. This also implies that the "outer" solution obtained by the grid moving method is accurate. To further justify this, another test is conducted. In the test, the boundary is retreated from II′ to II″ which is inside the large error region. It is found that due to the inaccurate boundary conditions (on II″), solution iterations are needed. After one cycle of solution iteration, the v velocity profile along the line II″ changes as is shown in Fig. 11a. This updated velocity profile remained unchanged in the following second and third cycles of iterations. On the other hand, the solution profile along the line II′ which is outside the large error regions remained the same in all the iteration cycles. These results imply that first, in this case the initial adaptive solution does provide an accurate solution in some areas of the domain. Second, the selection of the location of the boundary can be crucial to the efficiency of a procedure. The necessity of the "inner" and "outer" solution iteration is mainly determined by the accuracy of the internal boundary conditions instead of by the flow type (e.g., elliptic). If the internal boundaries are located in the low error regions, the effort spent on iteration can be minimized. The strategy for

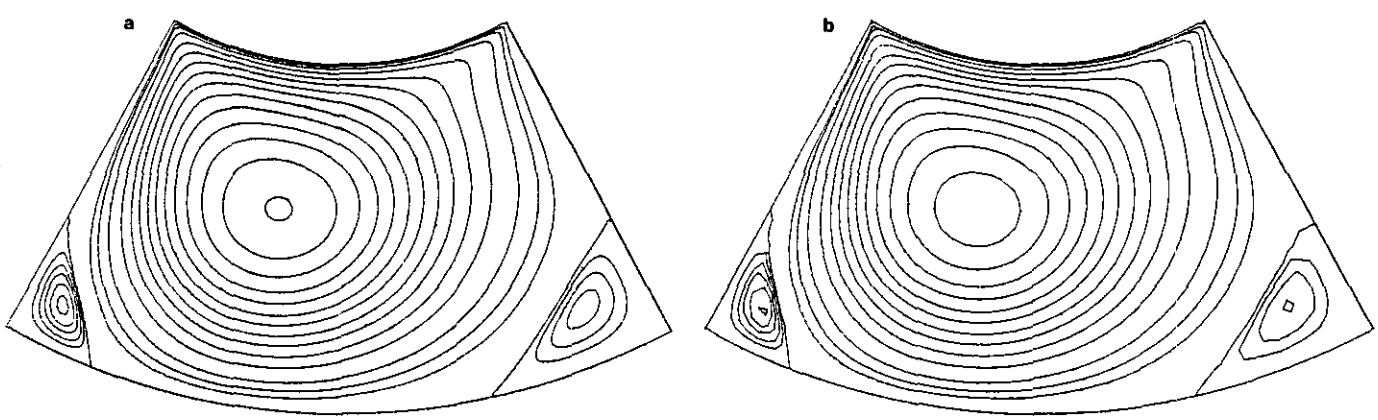

FIG. 13. The streamlines of the polar cavity flow: (a) based on 129 × 129 uniform grid solution; (b) based on 25-H adaptive grid solution.

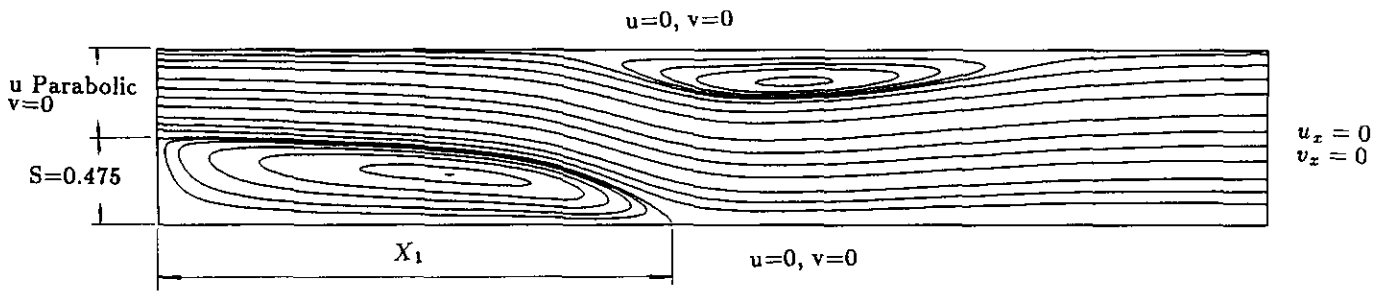

FIG. 14. The laminar backward facing step flow with the boundary conditions, Re = 800.

the choice of the boundary location is decisive especially when a multi-dimensional problem is to be solved. For a problem which needs many levels of grid refinement, solution iteration may require an enourmous effort.

The summary of the results is tabulated in Table III. The H grid and the HM grid are shown in Fig. 12. In this test problem, the HM grid is applied to the flagged region enclosed by the boundary II″ and the left wall (case 25-HM). On an HM grid, since all the grid points in the refined regions are dislocated after grid moving, heavy data sorting and interpolation along the boundaries are needed whenever the data are transferred. This will require some effort, especially in three-dimensional problems and when solution iterations and many levels of refinement are needed. For the present case, it is found that the advantage of using an HM grid is marginal. However, as mentioned before, an HM grid can be more effective in problems with high flow property gradients.

Table III compares the errors defined in Eqs. (12) and (13) among different approaches. The hybrid adaptive solution (25-H, 25-HM) errors are comparable to that of the 81×81 uniform fine grid solution (81-U) and the CPU time are reduced as much as 70 times. The total number of grid points used is about one-eighth of the latter. The storage requirement is therefore lower due to a smaller number of grid points. The table also shows that the grid moving solution (25-M) achieves the accuracy of a 41×41 uniform grid solution (41-U) with only one-fifth of the CPU time. Note that the improvement of the solution between the 25-M and 25-H is due to the reduced grid size in the refined regions. This step is effective since the grid refinement is conducted right in the large error regions, where the initial adaptive grid does not provide high enough resolution. It is interesting to note that the solution improvement between cases 25-M and 25-H is similar to that between cases 41-U and 81-U. In these cases the finest grid sizes (the last column in Table III), are also similar. The finest grid size achieved by the H grid is about 0.01 in either direction, this size is equivalent to two levels of halving the grid size on a 25×25 base grid. However, with two levels of grid refinement, the pattern recognition procedure and the data structure will be more complicated. This may cause significant extra effort in a three-dimensional problem. The total number of grid points used in the H grid is 882. Using a similar number of grid points in the grid moving method (31-M), the accuracy will be comparable to that of the 51-U. The streamline contour obtained by the hybrid method (25-H) is displayed in Fig. 13b in contrast to that based on the 129×129 grid solution (Fig. 13a).

3. Backward-Facing Step

In the second test flow problem, a laminar backward-facing step flow with Re = 800 as shown in Fig. 14 has been chosen. The Reynolds number is defined using the mean velocity in the inlet and twice its height as reference velocity and length, respectively. The step height is 0.475 and the inlet height is 0.5 so that the expansion ratio is 1.95 [34]. Note that the figure is not drawn to the scale; i.e., the channel height has been scaled up. The base grid is again 25×25 and the reference solution is a 101×101 uniform grid solution. After step 2 of the procedure, the grid-moving method yields the grid as shown in Fig. 15. The adaptive grids cluster near the free shear layer. Based on the moving grid

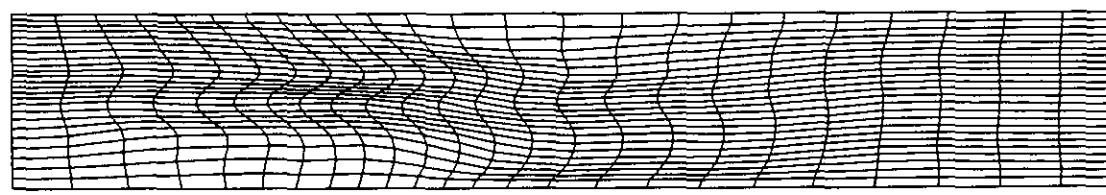

FIG. 15. The initial adaptive grid for the backward facing step flow.

solution, in the next figure, the large truncation error region acquired by Eq. (7) is compared to that obtained by using the Richardson method and by using the reference solution. To flag large error regions, the criteria, for the u component, are 0.05 in the reference solution approach, 0.05 in the Richardson method, and 15% in the formula approach. For the v component, they are 0.015, 0.015, and 15%, respectively. The normalized errors are defined previously. Note that large errors are concentrated near the free shear layer. The boundary for the large error region is marked as the solid line I in Fig. 16c. By extending the boundary line I two grid widths outward to I′, a similar effect of error reduction as shown in Fig. 10 for the cavity problem is observed. There is no need for solution iteration if the boundary I′ is chosen. This is demonstrated in the following test. Three boundary locations, that is, along the lines I′, I, and I″ as shown in Fig. 16c are tested. If the boundary is placed along the line I′, the solutions do not change after solution iteration. The v velocity component along the line I′ is shown in Fig. 17a which implies that the initial solution along the line I′ provides accurate boundary conditions for the refined region; therefore, no iteration is actually needed. On the other hand, if the boundary is retreated to the line I″ which is inside the large error region, iterations are required to correct the solutions. Figure 17b shows the solution change along the line I″ after the iteration. Note that only one cycle of solution iteration is needed to update the solutions. Theoretically, in an elliptic problem, a change in any part of the domain affects the solution elsewhere. However, the need for a solution iteration also depends on how strong the ellipticity is locally in the internal boundary. Take the limiting case as an example, if the boundary is placed very far downstream, where the flow resumes a fully developed one, no iteration shall be needed. At least numerically, the solution change after iteration will be negligible.

Based on the reference solution (101×101 uniform grid solution), the efficiencies of the various grids are compared in Table IV. The first row in the table is the numerical solution obtained by Guj and Stella [34]. A velocity–vorticity formulation, together with a grid of 40×101, was used in their study. The accuracy of the hybrid method solution (25-H) is comparable to that of the 81×81 uniform grid solution. However, the CPU time required is about 40 times less and the total number of grid points used is four times less. The solution by the grid moving method (25-M) also achieves the accuracy of that of a 41×41 uniform grid solution with only one-sixth of the CPU time. The case 41-M, which uses a similar total number of grid points with that of the hybrid method, can barely reach the accuracy of the hybrid grid solution with approximately two times more

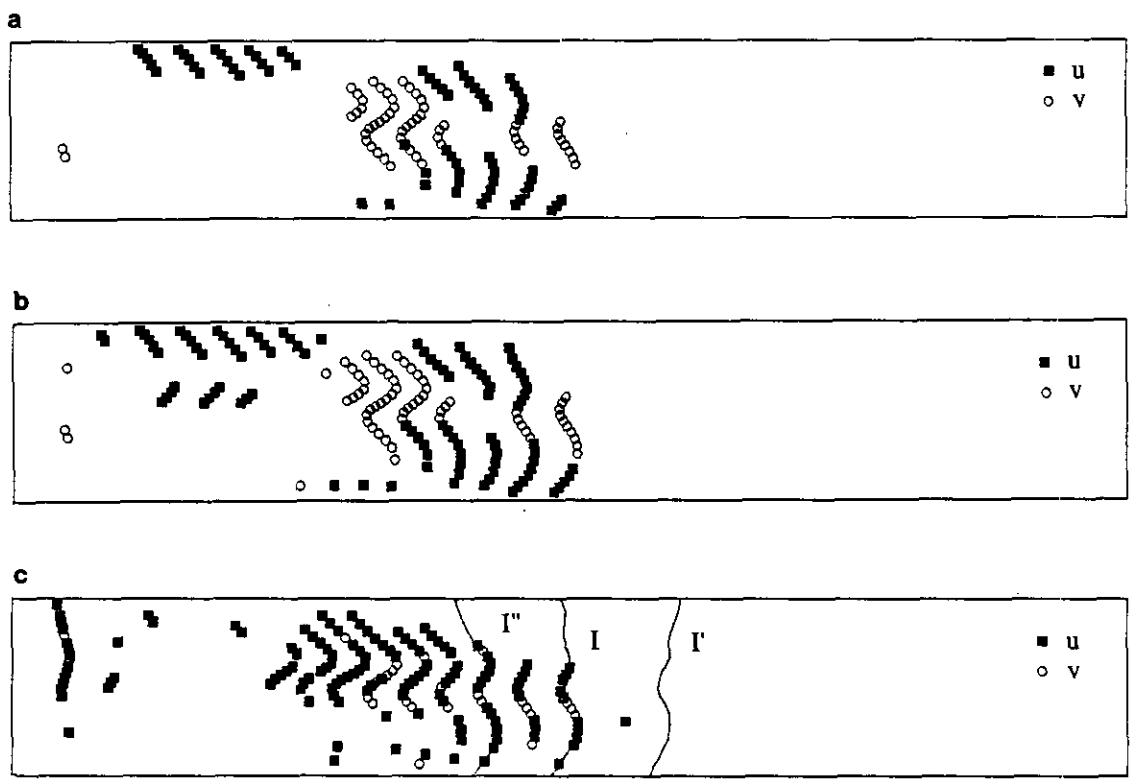

FIG. 16. Large error regions flagged by the various indicators: (a) solution errors relative to the reference solution (0.05 and 0.015 for the u, v components, respectively); (b) by the Richardson method (0.05, 0.015); (c) by the formula Eq. (7) (15%, 15%).

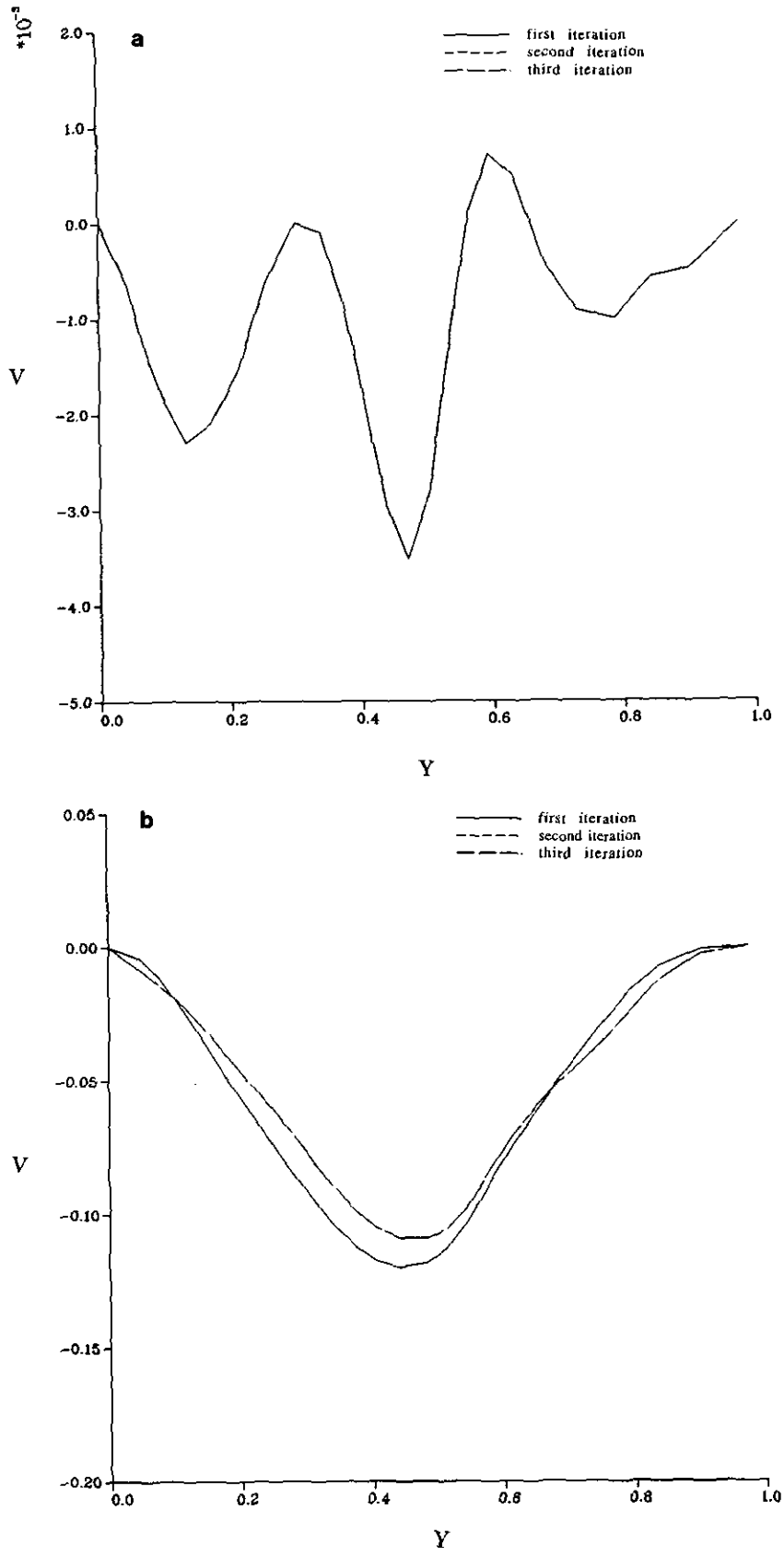

FIG. 17. The velocity profiles along the boundaries I″ and I′: (a) along I′; (b) along I″.

TABLE IV

Summary of the Performances of the Various Approaches (Backward Facing Step Flow)

Case	$X1/S$	ERR	ERR_M	CPU	Grid	G.S.(ξ, η)
Guj	12.0	—	—	—	4141	—
25-U	9.5	14.5	49.6	682	625	(0.52, 0.041)
25-M	11.8	3.5	15.3	720	625	(0.36, 0.020)
25-H	12.1	1.2	4.3	2101	1519	(0.18, 0.009)
41-U	10.6	5.6	18.1	4551	1681	(0.31, 0.024)
41-M	11.9	1.4	5.7	5011	1681	(0.20, 0.012)
61-U	11.7	2.4	8.0	15612	3721	(0.20, 0.016)
81-U	11.8	1.4	4.5	85445	6561	(0.16, 0.012)
101-U	12.0	—	—	321721	10201	(0.13, 0.010)

Note. U = uniform grid; M = adaptive grid, coupled; $ERR = (1/N)\sum_{i=1}^{N}[\sqrt{(u-u_0)^2+(v-v_0)^2}/\sqrt{u_0^2+v_0^2}]_i \times 100\%$; $ERR_M = \mathrm{Max}_{i=1}^{N}[\sqrt{(u-u_0)^2+(v-v_0)^2}/\sqrt{u_0^2+v_0^2}]_i \times 100\%$; where u, v are the coarse grid velocities, u_0, v_0 are 101×101 fine grid velocities, and N is the number of grid points.

CPU time. Since in this problem, the "outer" region does not need a finer grid, most grid points will be allocated in the shear layer region when the grid moving method is employed. In this sense, the distribution of the 41-M grid will be similar to that of the 25-H grid. This can explain why these two solutions are similar. Moreover, the hybrid adaptive grid has covered most of the domain in this case. The hybrid method is therefore more like a global method, viz., the grid moving method. The finest grid size obtained in the case 25-H is similar to that of the 81×81 uniform grid or, equivalently, two levels of halving the grid size from the base grid size. The finest grid sizes of the case 41-M are similar to those of the case 25-H.

From the results of the above test problems, it is seen that the present hybrid procedure improves the solution significantly. From both Tables III and IV, it is found that in our test cases, to achieve a similar accuracy, the efficiency of the hybrid method is higher than that of the moving grid method by a factor of two to three, together with a smaller total of grid points required. As mentioned previously, a direct comparison between a local refinement method and a global method is not practical. However, it is believed that the efficiency of a local refinement method is similar to that of the moving grid method [22]. This is partly supported by the results obtained in the present study. Several remarks on the effectiveness of the present procedure can be made. First of all, with a fixed initial number of grid points, the grid moving method provides relatively good resolution in large solution variation regions. This improved solution results in smaller large error regions. Second, local refinement further reduces errors by reducing the grid size right in the large error regions where more grid points are urgently needed. Note that in a traditional local refinement method which starts with a uniform base grid, more levels of refinement will be needed to achieve the same resolution as that of the hybrid method. Finally, since the total number of grid points used is much smaller than that used in a uniform grid solution, it is expected that the iteration number per grid node can be reduced significantly as discussed by Braaten and Shyy [35].

In the present hybrid method, only one level of refinement is applied. Nevertheless, the improvement of the solution is significant. If more than one level of refinement is needed, important issues such as pattern recognition and data structures should be studied further to facilitate the automation of the present procedure. From the viewpoint of engineering application, the present authors suggest that multi-level refinement should be avoided if possible, especially when applying to three-dimensional or transient problems, since complex pattern recognition procedure and data structure will detract from the effectiveness of the method. By the same token, a solution-iteration-free adaptive procedure is preferable; otherwise too many cycles of computation and interpolation will again reduce the efficiency of the method, especially in multi-dimensional problems. As demonstrated in the test cases, the Richardson method provides a reliable indicator. However, an adequate, direct estimator is still highly demanded for three-dimensional problems. Application of the present adaptive gridding procedure to three-dimensional problems is reported by the authors in another article [36].

SUMMARY

In the present study, an adaptive procedure which combines the concepts of global grid moving and local refinement has been devised. The truncation error formula derived previously is used as a direct error indicator to flag the large error regions. With adequate selection of the internal boundaries, iteration between the inner and outer solutions may not be needed. The specific efficiency of the procedure amounts to 40 and 70, respectively, in the two-dimensional test cases. The total number of grid points needed is only a fraction of that of a uniform grid case.

ACKNOWLEDGMENT

This study is funded by the National Science Council of Taiwan, Republic of China under Project NSC 79-0401-E006-34.

REFERENCES

1. J. F. Thompson, *Appl. Numer. Math.* 1, 3 (1985).
2. D. A. Anderson, "Adaptive Grid Methods for Partial Differential Equations," in *Advances in Grid Generation*, edited by K. N. Ghia and U. Ghia, FED, Vol. 5 (ASME, New York, 1983).

3. J. H. Ferziger, *J. Comput. Phys.* **69**, 1 (1987).
4. S. C. Caruso, J. H. Ferziger, and J. Oliger, AIAA Paper 86-0498, 1986 (unpublished).
5. M. J. Berger and J. Oliger, *J. Comput. Phys.* **53**, 484 (1984).
6. W. D. Gropp, *SIAM J. Sci. Stat. Comput.* **1**, 191 (1980).
7. R. J. Gelinas and S. K. Doss, *J. Comput. Phys.* **40**, 202 (1981).
8. D. C. Arney and J. E. Flaherty, *Appl. Numer. Math.* **5**, 257 (1989).
9. K. Y. Fung, J. Tripp, and B. Goble, *Comput. Methods Appl. Mech. Eng.* **66**, No. 1, 1 (1988).
10. W. Skamarock, J. Oliger, and R. L. Street, *J. Comput. Phys.* **80**, 27 (1989).
11. M. D. Smooke and M. L. Koszykowski, *J. Comput. Phys.* **62**, 1 (1986).
12. J. U. Brackbill and J. S. Saltzman, *J. Comput. Phys.* **46**, 342 (1982).
13. H. A. Dwyer, M. D. Smooke, and R. J. Kee, "Adaptive Gridding for Finite Difference Solutions to Heat and Mass Transfer Problems," in *Numerical Grid Generation*, edited by J. F. Thompson (North-Holland, Amsterdam, 1982).
14. D. Lee and W. Shyy, General Electric R & D Report 86CRD184, 1986 (unpublished).
15. W. Shyy, *Int. J. Numer. Methods Fluids* **8**, 475 (1988).
16. D. Lee and H. T. Lee, in *Proceedings, 5th Conference of the Chinese Society of Mechanical Engineering, Taipei, Taiwan, 1988*, p. 43.
17. D. Lee and Y. M. Tsuei, *Int. J. Numer. Methods Fluids* **14**, 775 (1992).
18. Y. N. Jeng and S. C. Liou, *Numer. Heat Transfer* **15**, 241 (1989).
19. A. T. Hsu, AIAA Paper 89-0006, Washington, DC, 1989 (unpublished).
20. D. Lee and Y. M. Tsuei, *Trans. Aeronaut. Astronaut. Soc. ROC* **22**, 1 (1989).
21. G. W. Hedstrom and G. H. Rodrique, in *Multigrid Methods*, Lecture Notes in Mathematics, Vol. 960 (Springer-Verlag, New York/Berlin, 1982).
22. J. F. Dannenhoffer III, in *Proceedings, 2nd Conf. on Numer. Grid Gen. in Comp. Fluid Mech.*, 1988, p. 319.
23. D. Lee, W. Shyy, and Y. M. Tsuei, in *Proceedings, International Symposium of Computational Fluid Dynamics, University of Sydney, Sydney, Australia, 1987*, edited by J. Noye and C. Fletcher (North Holland, Amsterdam, 1988), p. 401.
24. D. Lee and Y. M. Tsuei, *J. Comput. Phys. 98*, 90 (1992).
25. S. Acharya and F. H. Moukalled, *J. Comput. Phys.* **91**, 32 (1990).
26. S. V. Patankar, *Numerical Heat Transfer and Fluid Flow* (McGraw–Hill, New York, 1980).
27. G. Dahlquist and A. Bjorck, *Numerical Methods*, translated by N. Anderson (Prentice–Hall, Englewood Cliffs, NJ, 1974), Chap. 7.
28. M. C. Thompson and J. H. Ferziger, *J. Comput. Phys.* **82**, 94 (1989).
29. M. M. Rai, *J. Comput. Phys.* **62**, 472 (1986).
30. D. Lee and J. S. Lin, *Numer Heat Transfer* **20**, 65 (1991).
31. D. Lee and Y. C. Chao, Project Report CS76-0210-D006-21, National Science Council, Taiwan, ROC, 1988 (unpublished).
32. D. Lee, C. L. Yeh, Y. M. Tsuei and J. Chou, *J. Propulsion and Power* **9**, 322 (1993).
33. L. Fuchs and N. Tillmark, *Int. J. Numer. Methods Fluids* **5**, 311 (1985).
34. G. Guj and F. Stella, *Int. J. Numer. Methods Fluids* **8**, 405 (1988).
35. M. E. Braaten and W. Shyy, *Int. J. Numer. Methods Fluids* **6**, 559 (1986).
36. D. Lee and C. L. Yeh, *Comput. & Fluids*, in press.